Geophysical Analysis on Varthur Catchment Area, Bangalore Urban District, Karnataka, using Remote Sensing and GIS Techniques

Muni Krishna[1] , Saranya S[2] , Vajrappa H. C. [3]

ABSTRACT

Groundwater occurrence in hard rock terrains is governed by the geometry and interconnectedness of weathered and fractured zones in crystalline basement rocks (Dewandel et al., 2006; Maréchal et al., 2004). This study presents a geoelectrical investigation of the Varthur catchment, Dakshina Pinakini River Basin, Bengaluru, Karnataka, integrating Vertical Electrical Sounding (VES) with Dar Zarrouk parameter analysis and remote sensing GIS. A total of 46 VES stations were established across 284 km² using the Schlumberger configuration. Quantitative interpretation delineated a four-layer sequence comprising topsoil (ρ1: 12–65 Ω·m), weathered basement (ρ2: 22–157 Ω·m), fractured/partially weathered rock (ρ3: 84–535 Ω·m), and massive bedrock (Palacky, 1987), with weathered zone thickness (h2) ranging from 1.5–14.6 m (mean: 8.9 m). Longitudinal conductance (S: 0.09–0.51 S) indicated weak to moderate overburden protection at most stations, implying significant aquifer vulnerability (Henriet, 1976; Oladapo and Akintorinwa, 2007), while transverse resistance (T: 136.4–1581.7 Ω·m²) identified elevated groundwater potential in the southern and southeastern sectors (Niwas and Singhal, 1981; Utom et al., 2012). Structural contour analysis revealed heterogeneous basement depressions in the western and central portions. The integrated S–T interpretation demonstrates a trade-off between aquifer productivity and protective capacity typical of hard rock systems (Singhal and Gupta, 2010), providing a spatial framework for groundwater development and contamination risk management in this rapidly urbanizing catchment.

Keywords: Vertical Electrical Sounding | hard rock aquifer | Dar Zarrouk parameters | longitudinal conductance | transverse resistance | groundwater vulnerability

[1,2,3]Department of Geology, Bangalore University, Bangalore, India
Email: krishna.geo21@gmail.com

1 Introduction

Groundwater constitutes the primary source of freshwater for domestic, agricultural, and industrial supply across much of peninsular India, where crystalline hard rock formations underlie approximately 65% of the land surface (Dewandel et al., 2006; Singhal and Gupta, 2010). Unlike porous sedimentary aquifers, groundwater occurrence in these terrains is governed by secondary porosity and permeability developed through weathering and tectonic fracturing of the basement (Chandra et al., 2019; Prasad and Theophilus, 2009). The delineation of weathered and fractured zones in such heterogeneous media remains a fundamental challenge for sustainable groundwater resource management (Todd and Mays, 2005).

Geophysical resistivity methods have established themselves as the most cost-effective and field-deployable tools for subsurface characterization in crystalline terrains, owing to the high resistivity contrast between conductive weathered zones and resistive competent bedrock (Palacky, 1987; Yadav and Abolfazli, 1998). Vertical Electrical Sounding (VES), in particular, has been widely applied across sub-Saharan Africa, southern India, and semi-arid regions to delineate aquifer geometry, estimate saturated thickness, and evaluate groundwater potential (Acworth, 1987; Chandra et al., 2010; Dewandel et al., 2006). The quantitative interpretation of VES data through Dar Zarrouk parameters longitudinal conductance (S) and transverse resistance (T) provides additional hydrogeological insights into aquifer transmissivity and overburden protective capacity that cannot be obtained from layer thickness and resistivity alone (Henriet, 1976; Maillet, 1947; Niwas and Singhal, 1981).

The Varthur catchment, situated within the Dakshina Pinakini River Basin in the eastern fringe of Bengaluru, Karnataka, has experienced rapid urbanization over the past two decades, resulting in increased groundwater abstraction and elevated contamination risk to shallow crystalline aquifers. Despite its hydrogeological significance, systematic geoelectrical characterization of the subsurface in this catchment is lacking. Previous studies in the broader Bengaluru region have documented the utility of resistivity surveys for aquifer delineation (Shahid et al., 2000; Teeuw, 1995), but spatially comprehensive VES campaigns integrating Dar Zarrouk parameter analysis have not been reported for this specific catchment.

Hydrogeological studies in comparable Dharwar Craton settings have demonstrated that fracture density, aperture, and connectivity — rather than matrix porosity — determine productive well yields in hard rock terrains (Maréchal et al., 2004; Prasad and Theophilus, 2009). The integration of remote sensing and GIS with geophysical data has further improved groundwater potential mapping in such settings (Rajesh et al., 2012). The primary objectives of this study are: (i) to characterize the geoelectrical layer sequence and aquifer geometry across the Varthur catchment using 46 VES stations; (ii) to map the spatial distribution of weathered and fractured zone thicknesses; (iii) to evaluate aquifer protective capacity and groundwater potential through longitudinal conductance and transverse resistance analysis; and (iv) to identify priority zones for groundwater development and contamination management. The novelty of this contribution lies in the systematic spatial integration of Dar Zarrouk parameters with structural contour analysis in a rapidly urbanizing hard rock terrain where groundwater vulnerability assessment is urgently required.

2 Study Area

2.1 Location and Climate

The Varthur catchment is located in the southeastern part of Bengaluru Urban District, Karnataka, India, extending between latitudes 12°48′24.52″N and 12°53′59.85″N and longitudes 77°24′59.95″E and 77°30′6.72″E, encompassing an area of approximately 284 km² (Figure 1). The study area lies within the Dakshina Pinakini River Basin and is drained by the Varthur Lake system, which forms part of the interconnected Bellandur–Varthur lake chain. The topography is gently undulating, with elevations ranging from approximately 870 to 940 m above mean sea level.

The climate is semi-arid, classified under the Köppen–Geiger BSh category, receiving mean annual rainfall of approximately 900 mm distributed across two distinct monsoon seasons: the southwest monsoon (June–September) and the northeast monsoon (October–December). Average annual temperatures range from 16°C to 33°C. Recharge to the shallow crystalline aquifer system is primarily derived from monsoon precipitation and, increasingly, from return flows associated with urban water supply and wastewater disposal (Todd and Mays, 2005).

2.2 Geology and Hydrogeology

The Varthur catchment is underlain predominantly by Archaean crystalline basement comprising charnockite, hornblende–biotite gneiss, and granitic gneiss of the Dharwar Craton (Prasad and Theophilus, 2009). These rocks are generally massive, low in primary porosity, and exhibit variable degrees of secondary weathering and fracturing (Singhal and Gupta, 2010). The typical subsurface profile developed on these crystalline formations consists of: (i) a surficial lateritic and sandy topsoil horizon; (ii) a saprolitic weathered zone characterized by argillized feldspars and iron oxide enrichment; (iii) a partially fractured/partially weathered transitional zone; and (iv) a massive, relatively impermeable bedrock (Acworth, 1987; Dewandel et al., 2006).

Groundwater occurrence is predominantly confined to the basal saturated portion of the weathered zone and the underlying fractured rock horizon, consistent with the conceptual model of Dewandel et al. (2006) for granitic aquifers controlled by multiphase weathering. Bore wells in the area generally tap fractured gneissic formations at depths of 20–90 m below ground level, with reported yields of 0.5–5 L/s depending on fracture density and connectivity (Maréchal et al., 2004). The eastern and southeastern sectors of the catchment are characterized by deeper weathering profiles associated with lithological contrasts along gneissic foliation planes (Prasad and Theophilus, 2009).

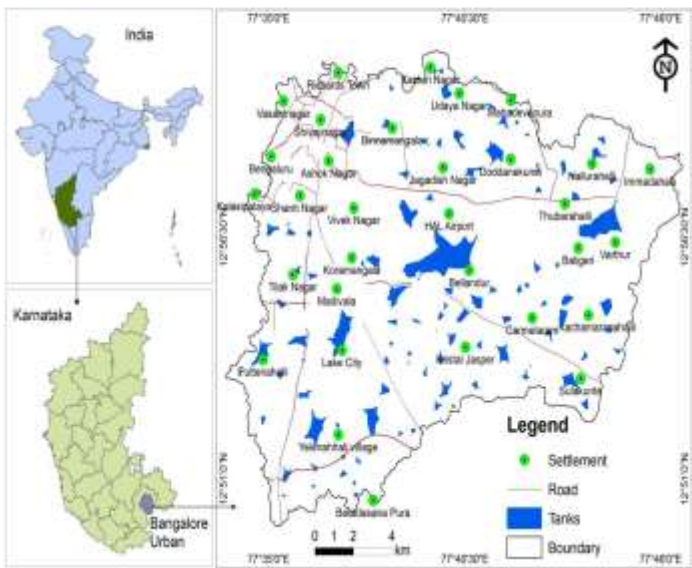

FIGURE 1 | Location map of the study area.

3 Materials and Methods

3.1 Electrical Resistivity Survey

Electrical resistivity soundings were conducted at 46 stations distributed across the study area (Figure 2) using the Schlumberger electrode configuration. Current electrode half-spacings (AB/2) were systematically expanded from 1.5 m to a maximum of 200 m to sample subsurface resistivity variations from near-surface to depths exceeding 60 m (Bhattacharya and Patra, 1968). Measurements were made using a calibrated resistivity meter (IGIS Model SSR-MP-ATS), and each sounding was repeated to ensure reproducibility. Additionally, apparent resistivity profiling was carried out at selected traverses using the Wenner configuration with electrode spacings of 50 m and 75 m to assess lateral resistivity variations at fixed investigation depths (Palacky, 1987).

3.2 Remote Sensing and GIS Analysis

Satellite imagery from Sentinel-2 (spatial resolution: 10 m) and SRTM digital elevation data (90 m resolution) were processed using ArcGIS 10.8 to produce base maps and to facilitate spatial interpolation of geoelectrical parameters (Rajesh et al., 2012). Land use/land cover classification was performed using maximum likelihood supervised classification. Drainage network extraction and catchment delineation were carried out from the DEM using watershed analysis tools (Teeuw, 1995).

3.3 VES Interpretation

Field resistivity sounding curves were initially interpreted using the curve-matching technique with master curves and auxiliary charts following Bhattacharya and Patra (1968). The preliminary layer models obtained from curve matching were refined through iterative computer-aided forward modelling using the IPI2WIN software (Bobachev et al., 2003), minimizing the root mean square error between observed and modelled apparent resistivity curves to below 5%. Borehole lithological data from three proximate wells were used for ground-truthing the interpreted geoelectrical layer models (Chandra et al., 2010).

3.4 Dar Zarrouk Parameters

Two fundamental Dar Zarrouk parameters were computed for each VES station following Maillet (1947) and Henriet (1976). Longitudinal conductance (S) is defined as:

$$S = \Sigma(h_i / \rho_i)$$

where hi and ρi are the thickness (m) and resistivity (Ω·m) of the ith layer, respectively. Transverse resistance (T) is defined as:

$$T = \Sigma(h_i \times \rho_i)$$

Longitudinal conductance provides a measure of overburden protective capacity against contaminant infiltration, with higher S values corresponding to greater protection (Henriet, 1976; Oladapo and Akintorinwa, 2007). Transverse resistance is empirically related to aquifer transmissivity in crystalline terrains through the relationship established by Niwas and Singhal (1981), and has been further validated by Utom et al. (2012) and Yadav and Abolfazli (1998) in comparable hard rock settings. The protective capacity classification followed Oladapo and Akintorinwa (2007): poor (<0.1 S), weak (0.1–0.2 S), moderate (0.2–0.4 S), and good (0.4–0.8 S).

3.5 Spatial Analysis and Mapping

Geoelectrical parameters (h1, h2, total thickness, S, T, apparent resistivity) were spatially interpolated using the kriging method in ArcGIS 10.8 to generate iso-parameter maps. Structural contour maps were prepared by subtracting the interpreted layer depths from the ground surface elevation derived from SRTM DEM, following the methodology of Twiss and Moores (1992). All maps were produced at a scale of 1:50,000.

FIGURE 2 | Location of Vertical Electrical Sounding (VES) stations in the study area.

4 Results

4.1 Geoelectrical Layer Characteristics

Interpretation of 46 VES sounding curves yielded predominantly four-layer geoelectrical sequences (H-type and K-type curves) across the study area, consistent with crystalline hard rock terrain profiles reported by Acworth (1987) and Singhal and Gupta (2010). The subsurface is characterised by a first layer corresponding to surficial topsoil (ρ1: 12–65 Ω·m; mean: 38.2 Ω·m; h1: 1.0–1.9 m; mean: 1.62 m), overlying a weathered crystalline basement (ρ2: 22–157 Ω·m; mean: 64.7 Ω·m; h2: 1.5–14.6 m; mean: 8.9 m). The third geoelectrical layer exhibits higher resistivity (ρ3: 84–535 Ω·m; mean: 200.4 Ω·m), interpreted as fractured to partially weathered basement rock (Palacky, 1987). A competent and resistive bedrock underlies these three units and constitutes the lowermost (undifferentiated) layer.

Borehole calibration at three locations confirmed the interpreted layer sequence: the VES-derived weathered zone thicknesses showed agreement within ±1.2 m of driller's logs, while the geoelectric third layer corresponded to fractured charnockite identified in drill cuttings (Chandra et al., 2010). The resistivity contrast between the weathered second layer and the resistive third layer enabled consistent layer discrimination across all 46 stations.

4.2 Weathered Zone Thickness

The thickness of the weathered zone (h2) exhibits significant spatial variability, ranging from 1.5 m (Kristal Jasper) to 14.6 m (Bommanahalli), with a mean of 8.9 m and standard deviation of 2.41 m. Anomalously thick weathered profiles (>12 m) are concentrated in the eastern and southeastern sectors of the catchment (Bommanahalli, Ashok Nagar, Mahadevapura), likely reflecting enhanced deep weathering along preferred lithological contacts and foliation planes within the gneissic basement (Dewandel et al., 2006; Prasad and Theophilus, 2009). In contrast, the central and northwestern portions of the study area are characterised by thinner weathered mantles (<8 m), indicative of less advanced weathering or truncation by erosional processes. The iso-thickness map of h2 (Figure 4) reveals several anomalous zones in the northern, western, central, and southeastern sectors, where lithological associations of weathered gneiss and granite provide enhanced infiltration capacity and groundwater storage (Acworth, 1987; Rajesh et al., 2012).

4.3 Fractured Zone Distribution

The third geoelectrical layer, interpreted as the fractured/partially weathered basement, exhibits a resistivity range of 84–535 Ω·m, with the highest values (>300 Ω·m) at Bellandur (535 Ω·m), Gunjur (385 Ω·m), Tilak Nagar (385 Ω·m), Iblur (386 Ω·m), and Venkatpura (380 Ω·m). These elevated third-layer resistivities are indicative of open, air- or freshwater-filled fractures within relatively fresh crystalline basement (Palacky, 1987; Singhal and Gupta, 2010), rather than clay-infilled or saturated zones. The fractured zone distribution (Figure 5), derived from structural contour analysis, suggests structural control by northeast–southwest trending foliation and joint sets consistent with regional Dharwar Craton tectonics (Prasad and Theophilus, 2009).

4.4 Structural Contour Analysis

Structural contour maps were constructed at the base of each geoelectrical layer by subtracting the cumulative layer depth from the surface DEM (Twiss and Moores, 1992). The structural contour at the base of the first geoelectric layer (Figure 3) closely mimics the shallow water table configuration, confirming hydraulic connectivity between the surficial topsoil and the underlying weathered zone. The contour map at the base of the second layer (Figure 4) reveals a more complex, heterogeneous subsurface configuration, with the maximum elevation difference between the northeastern (16 m) and southwestern (6 m) limits amounting to approximately 10 m. Numerous topographic closures on this surface, particularly in the western and central portions near Vembavur, indicate basement depressions that favour local groundwater accumulation (Maréchal et al., 2004) and are identified as priority targets for groundwater development.

4.5 Apparent Resistivity Distribution

Apparent resistivity maps generated for Wenner electrode spacings of a = 50 m and a = 75 m (Figure 6) reveal a pronounced north–south lateral variation in subsurface conditions (Palacky, 1987). In the northern sector, apparent resistivity contours at a = 50 m closely correspond to structural contours derived from VES interpretation, indicating shallow aquifer systems with moderate to high resistivity anomalies. Weaker correspondence between apparent resistivity and structural contours in the southern sector suggests the presence of deeper, more complex subsurface configurations, consistent with greater weathering depths and more heterogeneous fractured zones recorded in VES profiles (Chandra et al., 2010).

4.6 **Longitudinal Conductance (S)**

Computed longitudinal conductance values across the 46 VES stations range from 0.09 Siemens (Madivala; Cox Town) to 0.51 Siemens (Binnamangala), with a mean of 0.21 S (Table 1; Figure 7). The majority of stations (approximately 70%) fall within the weak to moderate protective capacity range (S = 0.1–0.3 S), following the classification scheme of Oladapo and Akintorinwa (2007). Very low values (S < 0.1 S) recorded at Madivala and Cox Town indicate negligible overburden protection, conferring high vulnerability of the underlying aquifer to contamination from surface sources — a critical concern given the dense urbanization of these localities (Todd and Mays, 2005). Moderate values (S = 0.2–0.3 S) recorded at JP Nagar, Shanti Nagar, and Richards Town reflect partial protection afforded by relatively thicker and more clay-rich weathered profiles (Henriet, 1976). The highest S value (0.51 S, Binnamangala) represents the only station classified as approaching good protective capacity in the study area, attributable to the presence of a clay-rich, well-developed saprolite (Acworth, 1987).

4.7 **Transverse Resistance (T)**

Transverse resistance values range from 136.4 Ω·m² (Kristal Jasper) to 1581.7 Ω·m² (Madivala), with a mean of 636.5 Ω·m² and a standard deviation of 297.8 Ω·m² (Table 1). Low T values (<300 Ω·m²) at Kristal Jasper and Binnamangala indicate poor aquifer potential, constrained by limited formation thickness or clay-rich lithology (Utom et al., 2012). Moderate T values (300–1000 Ω·m²) characterize. the largest portion of the study area, including Kalasipalaya, Adugodi, and Varthur, reflecting intermediate groundwater potential (Yadav and Abolfazli, 1998). High T values (>1000 Ω·m²) at Madivala (1581.7 Ω·m²), Bommanahalli (1299.8 Ω·m²), Cox Town (1195.4 Ω·m²), and Gunjur (1150.2 Ω·m²) indicate zones of elevated aquifer transmissivity (Niwas and Singhal, 1981), likely associated with thick fractured basement sections or intersections of multiple joint sets (Maréchal et al., 2004). The complete station-by-station VES dataset, including individual layer resistivities, thicknesses, and derived Dar Zarrouk parameters for all 46 stations, is provided in Table 1.

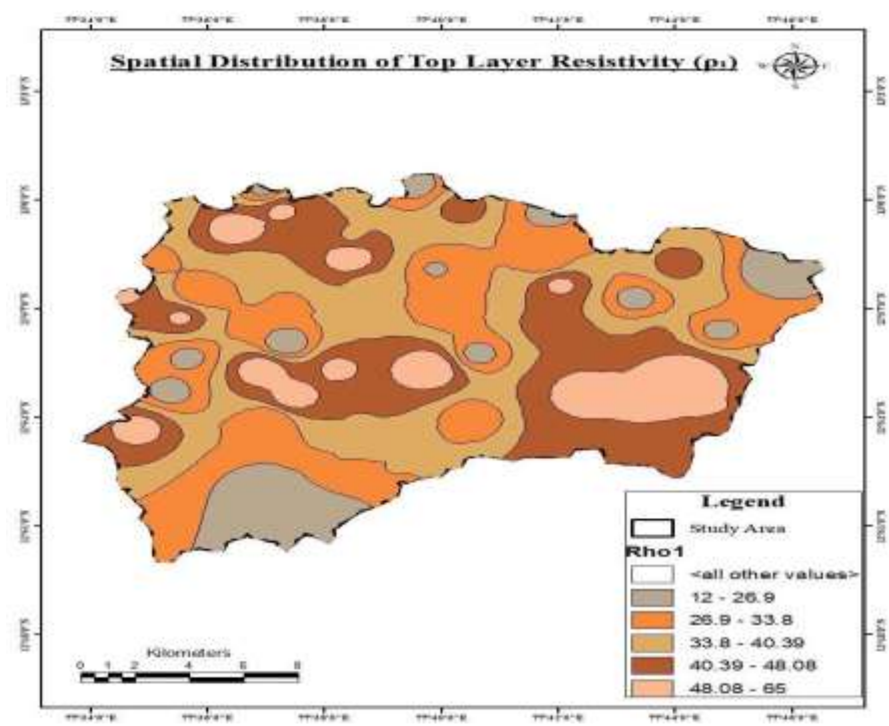

FIGURE 3 | Iso-thickness map at the base of the first geoelectric layer (depth in metres).

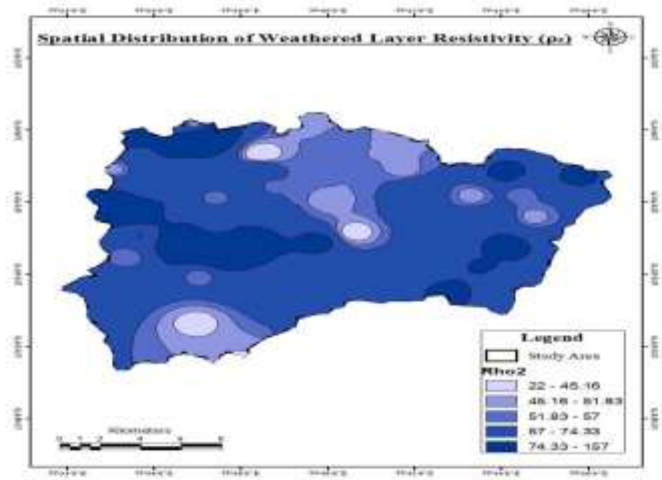

FIGURE 4 | Iso-thickness map at the base of the second geoelectric layer (depth in metres).

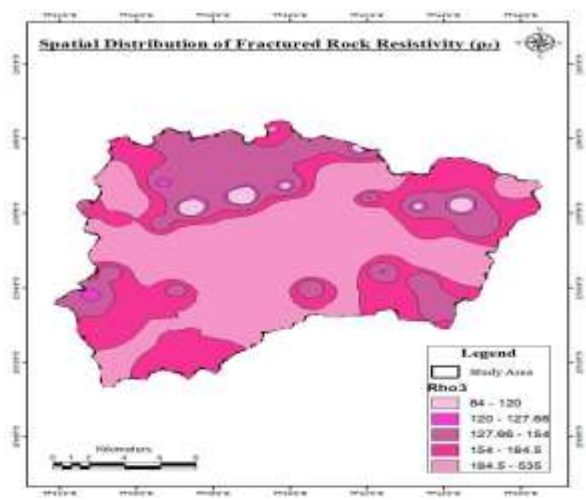

FIGURE 5 | Iso-thickness map at the base of the third geoelectric layer (depth in metres).

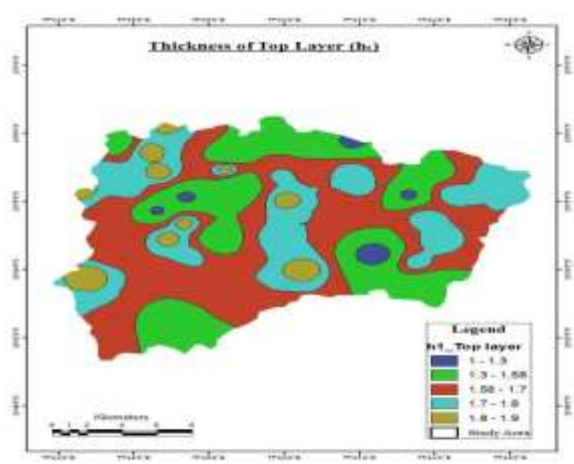

FIGURE 6 | Iso-apparent resistivity map for electrode separation a = 50 m.

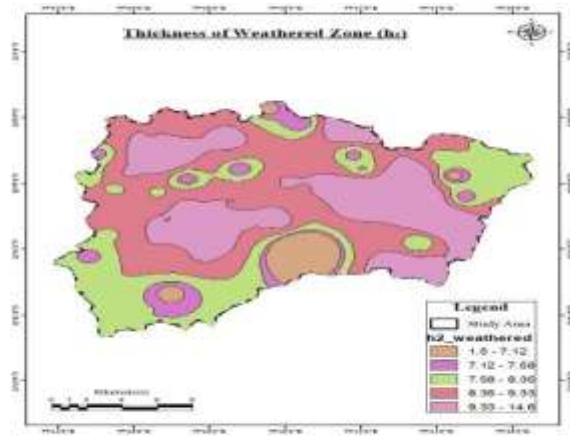

FIGURE 7 | Iso-apparent resistivity map for electrode separation a = 75 m.

5 Discussion

5.1 Aquifer Geometry and Groundwater Occurrence

The four-layer geoelectrical model identified across the Varthur catchment conforms to the conceptual stratification of crystalline aquifer systems proposed by Dewandel et al. (2006), wherein regolith is vertically partitioned into an upper saprolite (low resistivity, moderate storativity, low transmissivity) and a lower fractured zone (moderate to high resistivity, low storativity, high transmissivity). In the present study, the second geoelectrical layer ($\rho 2$: 22–157 Ω·m; mean h2: 8.9 m) is interpreted as the saturated saprolite aquifer, while the third layer ($\rho 3$: 84–535 Ω·m) represents the fractured crystalline horizon. The observed thickness range of h2 (1.5–14.6 m) is consistent with saprolite thicknesses reported for comparable Archaean crystalline terrains in Karnataka (10–30 m; Dewandel et al., 2006) and Tamil Nadu (5–25 m; Chandra et al., 2019), though the relatively thin profiles in this study likely reflect the peri-urban setting where saprolite has been partially removed or compacted by anthropogenic activities. Maréchal et al. (2004) demonstrated through multi-scale hydraulic testing that the fractured layer of hard rock aquifers is the primary contributor to borehole yield, a finding that is consistent with the high $\rho 3$ values observed in productive zones of the present study.

5.2 Hydrogeological Significance of Weathered and Fractured Zones

The inverse relationship between weathered zone resistivity ($\rho 2$) and clay content determines the hydraulic conductivity of the saprolitic aquifer (Chandra et al., 2019; Palacky, 1987). Low $\rho 2$ values (<40 Ω·m) at stations including Bengaluru (28 Ω·m), JP Nagar (21 Ω·m), and Immadahalli (15 Ω·m) may indicate clay-rich saprolite with reduced hydraulic conductivity, consistent with the findings of Chandra et al. (2019) who demonstrated that VES-derived resistivity can be used to estimate hydraulic conductivity in hard rock aquifers when calibrated against pumping test data. High third-layer resistivity ($\rho 3$ > 300 Ω·m) at Bellandur, Iblur, Gunjur, and Tilak Nagar suggests open fracture systems with minimal clay infilling, which are the most productive horizons for bore well development in hard rock terrains (Acworth, 1987; Singhal and Gupta, 2010).

The spatial distribution of fractured zones reveals partial structural control, with elevated resistivities aligned in a northeast–southwest orientation broadly consistent with the regional Dharwar foliation (Prasad and Theophilus, 2009). This structural alignment has been reported in regional hydrogeological studies across peninsular India (Dewandel et al., 2006; Prasad and Theophilus, 2009) and explains the observed clustering of high T values (>1000 Ω·m^2) in the southern and southeastern parts of the catchment where foliation-parallel jointing is better developed. Chandra et al. (2010) similarly observed that VES-derived small-scale resistivity variability in Archaean granitic aquifers correlates with fracture intensity mapping from borehole geophysical logs.

5.3 Groundwater Potential Assessment

The spatial distribution of transverse resistance values provides a first-order proxy for aquifer transmissivity, based on the theoretical relationship Taq ∝ T / ρw established by Niwas and Singhal (1981), where Taq is aquifer transmissivity and ρw is pore water resistivity. This relationship has been independently validated by Utom et al. (2012) in basement complex terrains of Nigeria and by Yadav and Abolfazli (1998) in semi-arid northwestern India. Zones with T > 1000 Ω·m² at Madivala, Bommanahalli, Cox Town, and Gunjur are interpreted as the most productive sectors for groundwater development, corresponding to areas where fractured gneissic or charnockitic formations underlie relatively thin saprolite. These zones are consistent with the locations of several existing high-yield bore wells in the eastern Bengaluru peri-urban belt, lending field corroboration to the geoelectrical interpretation.

Moderate T zones (300–1000 Ω·m²), which constitute approximately 60% of the study area, represent intermediate groundwater potential suitable for domestic and small-scale irrigation supply (Todd and Mays, 2005). The anomalously low T value at Kristal Jasper (136.4 Ω·m²; h2 = 1.5 m) reflects a site where the weathered zone is exceptionally thin and the underlying bedrock is compact, rendering it hydrogeologically unfavourable (Singhal and Gupta, 2010). Remote sensing and GIS integration in groundwater potential mapping (Rajesh et al., 2012; Teeuw, 1995) corroborates these geophysically derived assessments by linking surface lithological and structural signatures to sub-surface productive zones.

5.4 Aquifer Vulnerability and Protection Capacity

The predominantly low longitudinal conductance values (S < 0.3 S at approximately 85% of stations) indicate that the crystalline aquifer system in the Varthur catchment is characterized by weak overburden protection throughout most of the study area (Henriet, 1976; Oladapo and Akintorinwa, 2007). This is a direct consequence of the thin, coarse-grained saprolite developed on Archaean gneissic formations, which lacks the thick clay-rich horizons present in lateritized weathering profiles of more humid tropical terrains (Acworth, 1987). The critical implication for groundwater management is that contaminants introduced at the surface — including urban runoff, septic tank effluents, and leachate from unlined waste disposal sites — can migrate rapidly to the aquifer without significant attenuation (Todd and Mays, 2005).

The spatial coincidence of low S (< 0.1 S) and high T (> 1000 Ω·m²) values at Madivala and Cox Town identifies these areas as particularly critical from a groundwater protection standpoint: they are highly productive aquifer zones with negligible natural protection, representing maximum contamination risk in a context of dense urban land use. Similar inverse S–T relationships have been documented in hard rock terrains of southwestern Nigeria (Oladapo and Akintorinwa, 2007) and in basement complex aquifer systems studied by Utom et al. (2012) and Yadav and Abolfazli (1998), where low-conductance overburden overlies productive fractured aquifers.

5.5 Implications for Sustainable Groundwater Management

The geoelectrical data provide a spatially explicit framework for sustainable groundwater resource management in the Varthur catchment. Three management priorities are identified: First, groundwater development should be concentrated in zones of moderate to high T (>500 Ω·m²) in the southeastern and central sectors (Gunjur, Bommanahalli, Varthur Lake margins), where aquifer productivity is demonstrably higher (Niwas and Singhal, 1981; Utom et al., 2012). Second, groundwater quality monitoring programs should prioritize stations with S < 0.1 S, particularly in the urbanized northern and central localities

(Madivala, Cox Town), where contamination breakthrough to the aquifer is rapid (Henriet, 1976; Oladapo and Akintorinwa, 2007). Third, artificial recharge interventions (percolation ponds, check dams) should target zones with moderate weathered zone thickness (h2: 8–12 m) in the northern and western sectors, where available storage capacity and adequate saprolite thickness favor efficient recharge (Maréchal et al., 2004; Todd and Mays, 2005). Integration of the present geoelectrical data with hydrochemical analysis and land use mapping (Rajesh et al., 2012) would further improve the precision of vulnerability zoning for regulatory groundwater protection.

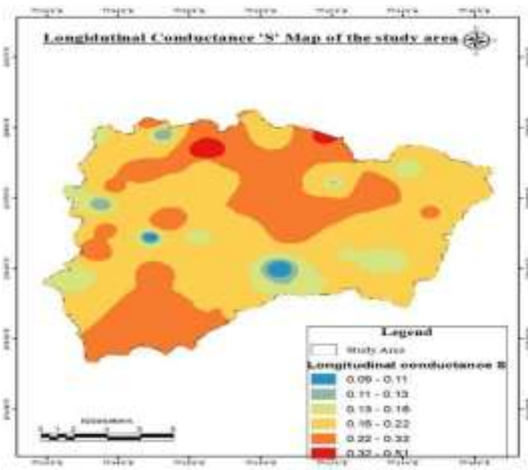

FIGURE 8 | Iso-longitudinal conductance (S) map of the study area.

6 Conclusion

A systematic geoelectrical investigation of the Varthur catchment, Dakshina Pinakini River Basin, using 46 Vertical Electrical Sounding stations has been carried out. The subsurface is characterized by a four-layer geoelectrical sequence comprising topsoil (ρ1: 12–65 Ω·m; h1: 1.0–1.9 m), weathered crystalline basement (ρ2: 22–157 Ω·m; h2: 1.5–14.6 m), fractured basement rock (ρ3: 84–535 Ω·m), and competent bedrock. This stratigraphy is consistent with the conceptual model of Dewandel et al. (2006) for granite aquifer systems. Weathered zone thickness (h2: mean 8.9 m) is greatest in the eastern and southeastern sectors, controlled by lithological contrasts along gneissic foliation planes (Prasad and Theophilus, 2009). Fractured zones with ρ3 > 300 Ω·m at Bellandur, Iblur, Gunjur, and Tilak Nagar represent the most productive aquifer horizons (Singhal and Gupta, 2010). Longitudinal conductance values (0.09–0.51 S; mean: 0.21 S) indicate weak to moderate overburden protective capacity across 85% of the study area (Oladapo and Akintorinwa, 2007), conferring high vulnerability of the crystalline aquifer to surface-derived contamination, especially in densely urbanized localities. Transverse resistance values (136.4–1581.7 Ω·m²) delineate zones of high groundwater potential in the southern and southeastern sectors (Madivala, Bommanahalli, Gunjur), consistent with structurally controlled fractured aquifer distribution (Niwas and Singhal, 1981). The spatial coincidence of high T and low S values at several urban stations (Madivala, Cox Town) identifies critical groundwater contamination risk zones that require priority monitoring and protective management

interventions (Henriet, 1976; Todd and Mays, 2005). Integration of geoelectrical data with structural contour analysis (Twiss and Moores, 1992) has identified basement depressions in the western and central portions of the catchment as favorable targets for artificial recharge and future groundwater development.

TABLE 1 | Layer parameters for the Vertical Electrical Sounding (VES) data.

VES ID	Location	ρ1 (Ω·m)	ρ2 (Ω·m)	ρ3 (Ω·m)	h1 (m)	h2 (m)	Total h (m)	S (Siemens)	T (Ω·m²)
1	Kalasipalaya	54	76	126	1.9	7.35	9.25	0.13	661.2
2	Puttenahalli	54	74	120	1.9	7.35	9.25	0.13	646.5
3	Bengaluru	28	46	365	1.8	7.2	9.0	0.22	381.6
4	JP Nagar	21	46	132	1.6	8.2	9.8	0.25	410.8
5	Vasantnagar	36	78	156	1.2	9.3	10.5	0.15	768.6
6	Siddapura	52	125	162	1.6	8.1	9.7	0.10	1095.7
7	Tilak Nagar	22	56	385	1.6	9.3	10.9	0.24	556.0
8	Shanti Nagar	22	56	226	1.8	9.5	11.3	0.25	571.6
9	Shivajinagar	62	78	156	1.9	9.3	11.2	0.15	843.2
10	Adugodi	32	63	126	1.2	8.1	9.3	0.17	548.7
11	Ashok Nagar	35	64	120	1.9	14.2	16.1	0.28	975.3

VES ID	Location	ρ1 (Ω·m)	ρ2 (Ω·m)	ρ3 (Ω·m)	h1 (m)	h2 (m)	Total h (m)	S (Siemens)	T (Ω·m²)
12	Madivala	64	157	248	1.9	9.3	11.2	0.09	1581.7
13	Richards Town	23	46	128	1.9	9.3	11.2	0.28	471.5
14	Yelenahahali Village	20	39	184	1.5	6.84	8.34	0.25	296.8
15	Lake City	22	47	132	1.6	8.1	9.7	0.25	415.9
16	Cox Town	52	135	152	1.7	8.2	9.9	0.09	1195.4
17	Koramangala	12	56	225	1.9	9.5	11.4	0.33	554.8
18	Vivek Nagar	32	51	84	1.2	6.84	8.04	0.17	387.2
19	Bommanahalli	57	82	224	1.8	14.6	16.4	0.21	1299.8
20	Betadasana Pura	12	44	152	1.5	7.6	9.1	0.30	352.4
21	Venkatpura	52	84	380	1.3	9.8	11.1	0.14	890.8
22	Indira Nagar	62	78	156	1.9	9.3	11.2	0.15	843.2
23	Binnamangala	39	22	132	1.3	10.4	11.7	0.51	279.5
24	Kodihalli	36	54	84	1.2	6.84	8.04	0.16	412.6
25	Kasturi Nagar	21	45	187	1.5	6.84	8.34	0.22	339.3
26	Iblur	64	85	386	1.8	10.2	12.0	0.15	982.2
27	Jagadish Nagar	25	53	112	1.75	8.5	10.25	0.23	494.3
28	HAL Airport	25	45	225	1.9	9.5	11.4	0.29	475.0
29	Udaya Nagar	46	54	126	1.5	6.8	8.3	0.16	436.2
30	Kristal Jasper	26	58	120	1.9	1.5	3.4	0.10	136.4
31	Bellandur	21	33	535	1.7	8.2	9.9	0.33	306.3
32	Doddanekundi	27	46	365	1.8	7.2	9.0	0.22	379.8
33	Mahadevapura	23	45	112	1.2	14.0	15.2	0.36	657.6
34	Tata Croma	46	65	270	1.6	14.2	15.8	0.25	996.6
35	Anand Nagar	53	74	122	1.8	7.4	9.2	0.13	643.0
36	Carmelaram	55	65	125	1.0	8.9	9.9	0.16	633.5
37	Kodathi	45	84	165	1.6	11.0	12.6	0.17	996.0
38	Thubarahalli	20	45	112	1.2	12.0	13.2	0.33	564.0
39	Mullur	53	77	125	1.8	7.21	9.01	0.13	650.6
40	Baligeri	42	74	164	1.8	11.3	13.1	0.20	911.8
41	Sulakunte	41	56	132	1.3	9.6	10.9	0.20	590.9
42	Nallurahalli	46	85	166	1.5	8.1	9.6	0.13	757.5
43	Gunjur	65	84	385	1.8	12.3	14.1	0.17	1150.2
44	Ramagondana halli	36	52	96	1.8	6.7	8.5	0.18	413.2
45	Varthur	22	46	128	1.7	7.11	8.81	0.23	364.5
46	Immadahalli	15	78	200	1.8	7.51	9.31	0.22	612.8

References

Acworth, R. I. 1987. “The Development of Crystalline Basement Aquifers in a Tropical Environment.” Quarterly Journal of Engineering Geology 20, no. 4: 265–272. https://doi.org/10.1144/GSL.QJEG.1987.020.04.02.

Bhattacharya, P. K., and H. P. Patra. 1968. Direct Current Electric Sounding. Methods in Geochemistry and Geophysics, vol. 10. Amsterdam: Elsevier. https://doi.org/10.1016/C2013-0-14672-3.

Bobachev, A. A., I. N. Modin, and V. A. Shevnin. 2003. “IPI2Win: A Windows Software for an Automatic Interpretation of Resistivity Sounding Data.” Moscow State University, Moscow. http://geophys.geol.msu.ru/ipi2win.htm.

Chandra, S., S. Ahmed, A. Ram, and B. Dewandel. 2019. “Estimation of Hard Rock Aquifer Hydraulic Conductivity From Geoelectrical Measurements: A Theoretical Development With Field Application.” Journal of Hydrology 570: 40–52. https://doi.org/10.1016/j.jhydrol.2018.12.065.

Chandra, S., B. Dewandel, S. Dutta, and S. Ahmed. 2010. “Geophysical Model of Geological Discontinuities in a Granitic Aquifer: Analyzing Small Scale Variability of Electrical Resistivity for Groundwater Occurrences.” Journal of Applied Geophysics 71, no. 4: 137–148. https://doi.org/10.1016/j.jappgeo.2010.06.003.

Dewandel, B., P. Lachassagne, R. Wyns, J. C. Maréchal, and N. S. Krishnamurthy. 2006. “A Generalized 3-D Geological and Hydrogeological Conceptual Model of Granite Aquifers Controlled by Single or Multiphase Weathering.” Journal of Hydrology 330: 260–284. https://doi.org/10.1016/j.jhydrol.2006.03.026.

Henriet, J. P. 1976. “Direct Applications of the Dar Zarrouk Parameters in Groundwater Surveys.” Geophysical Prospecting 24, no. 2: 344–353. https://doi.org/10.1111/j.1365-2478.1976.tb00931.x.

Maillet, R. 1947. “The Fundamental Equations of Electrical Prospecting.” Geophysics 12, no. 4: 529–556. https://doi.org/10.1190/1.1437322.

Maréchal, J. C., B. Dewandel, and K. Subrahmanyam. 2004. “Use of Hydraulic Tests at Different Scales to Characterize Fracture Network Properties in the Weathered-Fractured Layer of a Hard Rock Aquifer.” Water Resources Research 40: W11508. https://doi.org/10.1029/2004WR003137.

Niwas, S., and D. C. Singhal. 1981. “Estimation of Aquifer Transmissivity From Dar Zarrouk Parameters in Porous Media.” Journal of Hydrology 50: 393–399. https://doi.org/10.1016/0022-1694(81)90082-2.

Oladapo, M. I., and O. J. Akintorinwa. 2007. “Hydrogeophysical Study of Ogbese Southwestern Nigeria.” Global Journal of Pure and Applied Sciences 13, no. 1: 55–61. https://doi.org/10.4314/gjpas.v13i1.16669.

Palacky, G. J. 1987. “Resistivity Characteristics of Geologic Targets.” In Electromagnetic Methods in Applied Geophysics, vol. 1, edited by M. N. Nabighian, 53–129. Tulsa: Society of Exploration Geophysicists. https://doi.org/10.1190/1.9781560802631.ch3.

Prasad, K. N., and A. Theophilus. 2009. “Hydrogeological Framework of Weathered Basement Aquifers in the Dharwar Craton: Implications for Groundwater Development.” Hydrogeology Journal 17, no. 7: 1737–1750. https://doi.org/10.1007/s10040-009-0468-7.

Rajesh, R., B. V. S. Murthy, and S. Rajesh. 2012. “A Novel Approach to Delineate Groundwater Potential Zones Using Remote Sensing and GIS in Hard Rock Terrain.” Water Resources Management 26, no. 14: 4025–4041. https://doi.org/10.1007/s11269-012-0126-9.

Shahid, S., S. K. Nath, and H. P. Patra. 2000. “Ground Water Assessment and Management Within Typical Laterites Around Salboni, District Midnapur (W.B.).” Journal of Indian Water Works Association 32, no. 2: 101–106.

Singhal, B. B. S., and R. P. Gupta. 2010. Applied Hydrogeology of Fractured Rocks. 2nd ed. Dordrecht: Springer. https://doi.org/10.1007/978-90-481-8799-7.

Teeuw, R. M. 1995. “Groundwater Exploration Using Remote Sensing and a Low-Cost Geographical Information System.” Hydrogeology Journal 3, no. 3: 21–30. https://doi.org/10.1007/s100400050050.

Todd, D. K., and L. W. Mays. 2005. Groundwater Hydrology. 3rd ed. Hoboken, NJ: John Wiley & Sons.

Twiss, R. J., and E. M. Moores. 1992. Structural Geology. San Francisco: W. H. Freeman & Co.

Utom, A. U., B. I. Odoh, and A. U. Okoro. 2012. “Estimation of Aquifer Transmissivity Using Dar Zarrouk Parameters Derived From Surface Resistivity Measurements: A Case History From Parts of Enugu Town (Nigeria).” Journal of Water Resource and Protection 4, no. 12: 993–1000. https://doi.org/10.4236/jwarp.2012.412115.

Yadav, G. S., and H. Abolfazli. 1998. “Geoelectrical Soundings and Their Relationship to Hydraulic Parameters in Semi-Arid Regions of Jalore, Northwestern India.” Journal of Applied Geophysics 39, no. 1: 35–51. https://doi.org/10.1016/S092.